Catalysis Today 164 (2011) 515–519

Contents lists available at ScienceDirect

Catalysis Today

journal homepage: www.elsevier.com/locate/cattod

Aromatic hydrocarbons and sulfur based catalyst deactivation for selective catalytic reduction of NO_x

Vladimir Demidyuk[a], Christopher Hardacre[a], Robbie Burch[a], Ashish Mhadeshwar[b,1], Daniel Norton[b], Dan Hancu[b,*]

[a] CenTACat/School of Chemistry and Chemical Engineering, Queen's University Belfast, Belfast BT9 5AG, UK
[b] General Electric Global Research Center, 1 Research Circle, Niskayuna, NY 12309, USA

ARTICLE INFO

Article history:
Received 1 July 2010
Received in revised form
22 December 2010
Accepted 25 December 2010
Available online 17 February 2011

Keywords:
SCR
NO_x
Hydrocarbon
Silver
Deactivation
Aromatics
Sulfur

ABSTRACT

Chemical deactivation of Ag/Al_2O_3 catalysts due to aromatic species and sulfur present in the diesel fuel is a major challenge in hydrocarbon-based selective catalytic reduction (HC-SCR) of NO_x from diesel engine exhaust. In this paper, mechanisms for catalyst deactivation due to both aromatic species and sulfur are investigated using model hydrocarbon species, such as toluene and xylene, as well as sulfation treatment. A number of experimental techniques, viz., microreactor studies, temperature programmed oxidation, temperature programmed decomposition, and diffuse reflectance UV–vis, are employed to understand the contribution of aromatic species and sulfur to catalyst deactivation. It is observed that the inhibition effect due to aromatic species is reversible, but is dependent on the size and concentration of the aromatic species. The sulfation effect is irreversible at a given temperature, and sulfur not only reacts with the silver particles, but also affects the relative magnitude of the different types of hydrocarbon species adsorbed on the catalyst surface, thereby changing the catalytic activity for the SCR chemistry.

1. Introduction

The selective catalytic reduction (SCR) of NO_x by hydrocarbons (HC) has attracted great attention as a promising method for the removal of environmentally hazardous NO_x emissions from diesel engine exhaust. Significant research work has been published over the last decade, focusing on catalyst preparation and SCR mechanism investigation [1–9]. The most commonly explored catalyst for HC-SCR is silver supported on alumina (Ag/Al_2O_3).

Use of onboard diesel fuel for NO_x reduction offers a significant advantage over urea-based SCR systems [10–12], as no separate infrastructure development is required. However, a major challenge for HC-SCR is the inhibitory effect by aromatic species and long-chain alkanes present in the diesel fuel [13–15]. Both components promote coke formation on the catalyst surface, resulting in gradual degradation in the SCR performance [6]. Empirical attempts to reduce the effect of aromatics involve optimized fuel injection [6]; therefore, it is important to develop a detailed understanding of this inhibiting effect. Furthermore, typical silver-based catalysts are susceptible to poisoning with sulfur oxides, which originate from the oxidation of sulfur in the diesel fuel. Several authors have demonstrated such catalyst deactivation in the presence of SO_2 [16–19]. On the other hand, other authors have reported a promotional effect with SO_2 [20,21], with some describing a shift in the NO_x conversion window to higher temperature, which results in an increase in NO_x conversion at higher temperature but a reduced NO_x conversion at lower temperature [22,23].

In the current work, a range of experimental techniques have been used, some for the first time, with the aim of establishing the mechanism of inhibition by aromatic species and deactivation by sulfur for the HC-SCR of NO_x on Ag/Al_2O_3 catalyst.

2. Experimental

Alumina-supported silver catalysts were prepared using incipient wetness with silver nitrate as the precursor. γ-Alumina (Norton) support with a surface area of ~200 m^2/g was used. Catalysts with loadings of 2 wt.% and 3 wt.% Ag were prepared. Testing was performed using a micro-reactor, which consisted of a heated quartz tube (3 mm i.d.). The catalyst sample (0.2 g, particle size of 250–425 μm) was exposed to a full gas mixture at a flow rate of 200 cm^3/min, comprising 300 ppm NO, 300 ppm CO, 7 vol.% H_2O, 12 vol.% O_2, 6 vol.% CO_2, and He in balance (BOC Gases, UK). Octane,

* Corresponding author. Tel.: +1 518 387 5011; fax: +1 518 387 5592.
E-mail address: hancuda@crd.ge.com (D. Hancu).
[1] Department of Chemical, Materials, and Biomolecular Engineering, University of Connecticut, Storrs, CT 06269, United States.

0920-5861/$ – see front matter © 2011 Elsevier B.V. All rights reserved.
doi:10.1016/j.cattod.2010.12.047

toluene, and para-xylene were used as the hydrocarbon reductants, with total concentration of 1800 ppm on a C_1 basis (i.e., a C_1:NO_x ratio of 6 was used). A chemiluminescence NO_x detector (Signal series 4000) was used for the analysis of NO and NO_2, and a mass spectrometer (Pfeiffer OmniStar-301) was used to analyze CO_2, CO/N_2, octane, toluene, xylene, and H_2O. NO_x conversion was typically measured after 60 min at constant temperature starting from 425 °C and decreasing the temperature in 25 °C intervals. Temperature-programmed oxidation (TPO) experiments were carried out in 10% O_2/Ar and temperature-programmed decomposition (TPD) experiments were performed in Ar both with a ramp rate of 5 °C/min from ambient temperature to 700 °C directly after the reaction. To investigate the combined effect of aromatic species and sulfur in the fuel, experiments were conducted after a sulfation pretreatment at 450 °C for 6 h using 30 ppm SO_2, 7 vol.% H_2O, and 12 vol.% O_2.

3. Results and discussion

3.1. Aromatic inhibition effect

SCR experiments were carried out using octane and toluene as representative hydrocarbon reductants. Fig. 1 shows the NO_x conversion for the (a) 2% Ag/Al_2O_3 and (b) 3% Ag/Al_2O_3 catalysts as a function of temperature for octane, toluene, and a mixture of 29% toluene and 71% octane. It is clear that the presence of toluene significantly decreases the octane-SCR performance, but these activity tests cannot explain whether such decrease is because of inherently lower toluene-SCR activity or catalyst site inhibition from toluene.

To explore this issue, a small amount of toluene was injected to the octane-SCR reaction. Fig. 2 shows the inhibiting effect of toluene on NO_x reduction by octane. Immediately after the toluene injection, there is a sharp rise in NO concentration (i.e., a decrease in the NO_x conversion) before the conversion recovers to the original steady state value after ~15 min. Furthermore, as the amount of toluene injected increases from 0.01 cm^3 to 0.03 cm^3 the overall extent of inhibition (area under the curve and the time required to recover the original steady state NO concentration) also increases. For example, the areas under the curves for injection of 0.01 cm^3 vs. 0.02 cm^3 toluene are 126 ppm-min and 238 ppm-min, respectively. In addition, upon toluene injection, a sharp peak is observed in the octane signal shown in Fig. 3 indicating that toluene competes with octane for adsorption sites on the catalyst. Since this occurs simultaneously with the loss of NO_x reduction performance in Fig. 2, it appears that toluene is adsorbing on the Ag sites responsible for the HC-SCR chemistry. Toluene injection does not lead to CO_2 formation even at high temperature (400 °C), therefore the recovered performance should be due to toluene desorption. Injection tests conducted at different temperatures showed that higher temperature decreases the inhibition effect, which could be due to increased mobility or desorption of the aromatic species. Similar experiments using xylene show that xylene is an even stronger inhibitor than toluene, as shown in Fig. 4. The overall extent of inhibition (area under the curve and the time required to recover the original steady state NO concentration) is also higher for xylene (area = 353 ppm-min) than that for toluene (area = 98 ppm-min) despite the fact that ~20% fewer moles of xylene were injected than toluene.

This competitive adsorption is supported by the TPO results in Fig. 5, which shows that the amount of carbon on the surface increases in the order: octane < toluene < xylene, even though the total hydrocarbon concentration is the same (1800 ppm on C_1 basis) in all cases. On the other hand, the TPD profiles for CO_2 presented in Fig. 6 show that the aromatic hydrocarbons modify the nature of the adsorbed surface hydrocarbons. In case of octane, there are two CO_2 peaks at ~425 °C and ~575 °C, which are similar in size

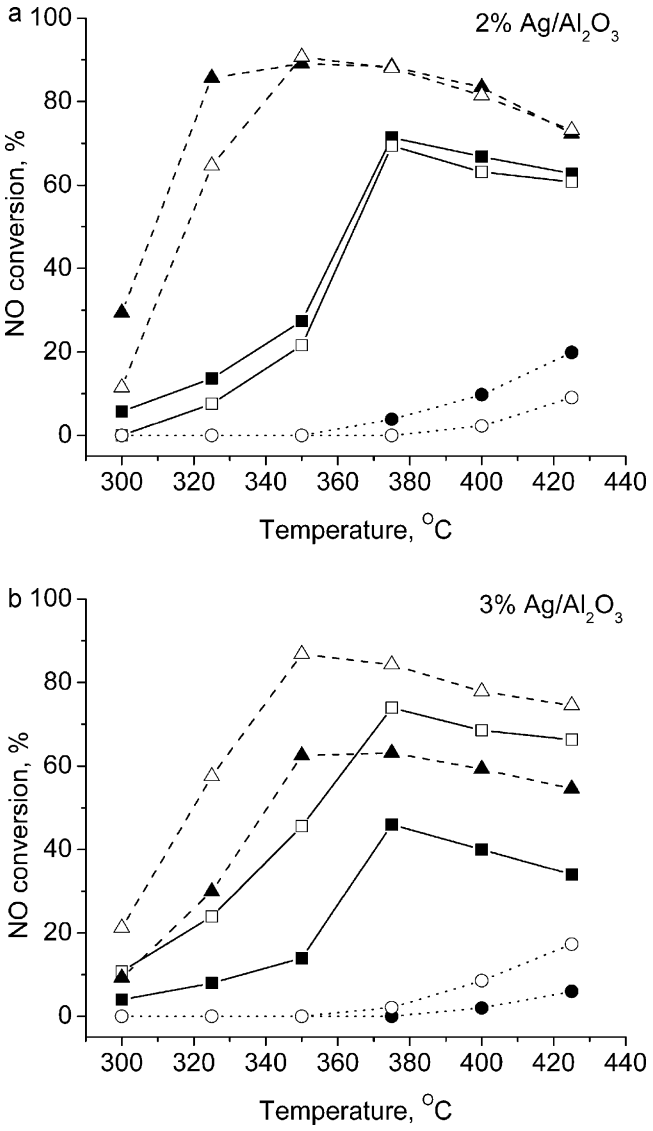

Fig. 1. NO_x conversion as a function of temperature for (a) 2% Ag/Al_2O_3 and (b) 3% Ag/Al_2O_3 catalysts. Catalysts were tested at 200 cm^3/min. Initial gas composition was 300 ppm NO, 300 ppm CO, 7 vol.% H_2O, 12 vol.% O_2, 6 vol.% CO_2, and He in balance. C_1:NO ratio was 6. (▲) Octane; fresh catalyst, (△) octane; sulfated catalyst, (■) octane + toluene; fresh catalyst, (□) octane + toluene; sulfated catalyst, (●) toluene; fresh catalyst, (○) toluene; sulfated catalyst.

resulting from the decomposition of partially oxidized hydrocarbon species on the surface. With addition of toluene, magnitude of the first peak slightly decreases, whereas addition of xylene nearly eliminates it.

3.2. Sulfur effect

Fig. 1 shows the effect of sulfation pretreatment on the NO_x conversion. For both catalyst loadings, a significant change was observed in the NO_x conversion performance. Sulfur poisoning is often irreversible and cumulative, unlike aromatic species inhibition, which is a reversible effect, as seen from Figs. 2 and 4. For the 2% Ag/Al_2O_3 catalyst, the NO_x conversion is not affected by sulfation at higher temperature, but decreases at lower temperature, as compared to the performance results before sulfation. On the other hand, for the 3% Ag/Al_2O_3 catalyst, NO_x conversion is low before sulfation, but it significantly increases after the sulfation pretreatment. This is similar to the results reported previously [16–18,20–23].

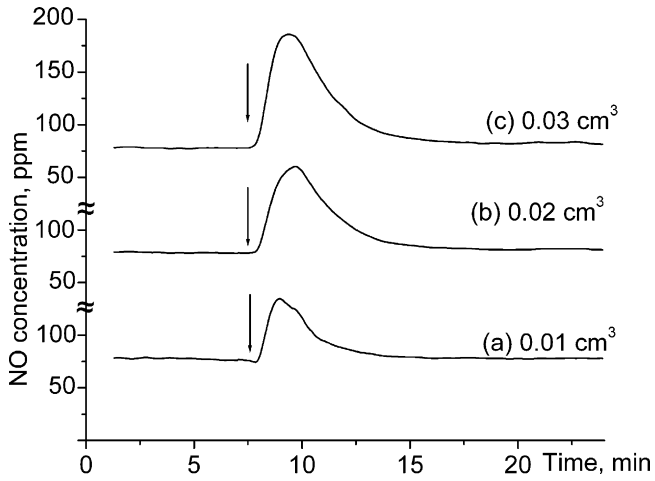

Fig. 2. Effect of toluene injection on NO reduction over 2% Ag/Al_2O_3 at 400 °C with (a) 0.01 cm^3, (b) 0.02 cm^3, and (c) 0.03 cm^3 of injected toluene. Arrows correspond to injection of toluene. Initial NO concentration was 300 ppm and steady-state NO concentration before toluene injection was 80 ppm. Operating conditions are the same as in Fig. 1.

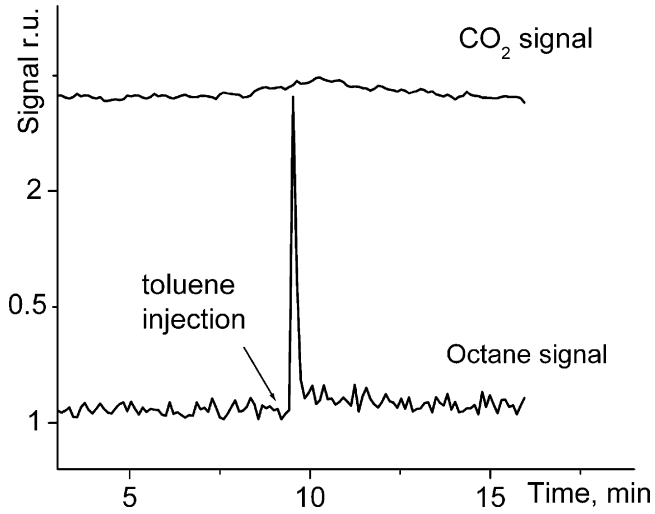

Fig. 3. Effect of toluene injection on octane and CO_2 profiles. Initial CO_2 concentration was 0 ppm. Remaining operating conditions are the same as in Fig. 1.

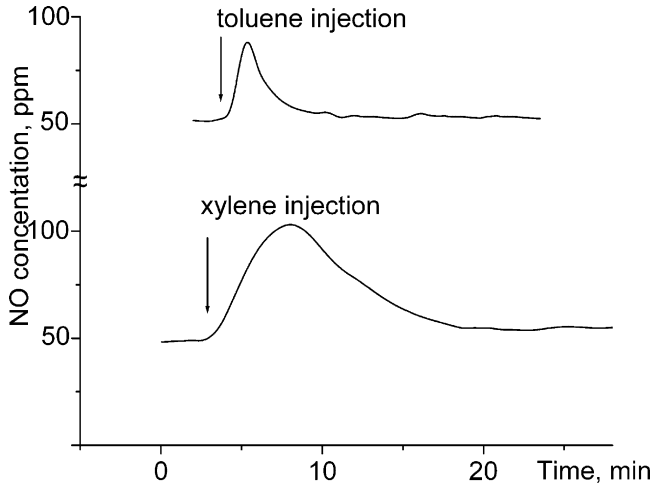

Fig. 4. Effect of 0.01 ml toluene and 0.01 ml xylene injection on NO reduction over 2% Ag/Al_2O_3 at 350 °C. Initial NO concentration was 300 ppm and steady-state NO concentration before toluene or xylene injection was 45 ppm. Operating conditions are the same as in Fig. 1.

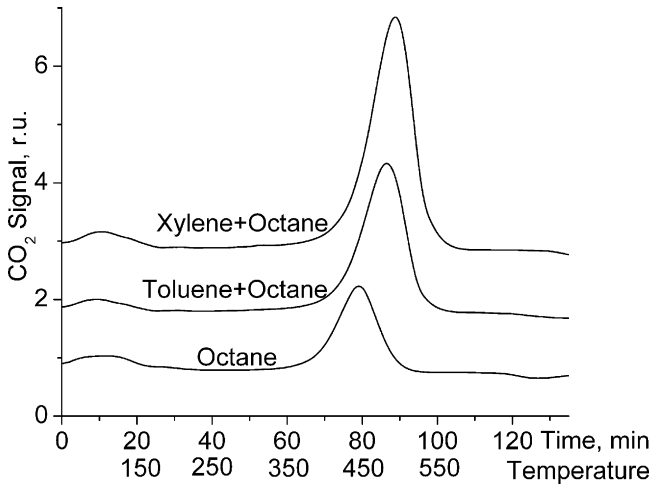

Fig. 5. Temperature-programmed oxidation profiles for used 2% Ag/Al_2O_3 catalyst samples. Catalyst was tested with octane, mixture of 29% toluene and 71% octane, as well as mixture of 29% p-xylene and 71% octane; at 300 °C for 4 h. Operating conditions are the same as in Fig. 1.

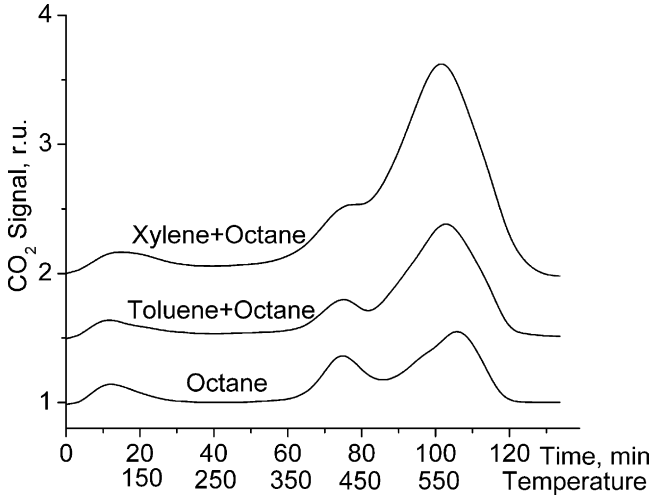

Fig. 6. Temperature-programmed decomposition profiles for used 2% Ag/Al_2O_3 catalyst samples. Catalyst was tested with octane, mixture of 29% toluene and 71% octane, as well as mixture of 29% p-xylene and 71% octane; at 300 °C for 4 h. Operating conditions are the same as in Fig. 1.

Fig. 7a shows that in case of the 2% Ag/Al_2O_3 catalyst, toluene injection has a much larger inhibition effect for a sulfated catalyst compared to that for the fresh catalyst. As shown in Fig. 7b, the 3% Ag/Al_2O_3 catalyst, which appears more tolerant to toluene inhibition before the sulfation treatment, also shows significant deactivation after the sulfation process. Sulfation converts the silver particles that are responsible for oxidizing the hydrocarbons into silver sulfate. Previous reports indicate that Ag_2SO_4 in combination with Ag clusters exhibit SCR activity [21]. Therefore, the net result is an increase in the overall SCR performance due to better hydrocarbons utilization in the SCR chemistry, and a decrease in tolerance towards toluene inhibition. It is expected that this effect would diminish upon deeper sulfation when both the alumina support and smaller silver clusters are converted to the corresponding sulfated species.

The diffuse reflectance UV–vis spectra of catalysts are shown in Fig. 8 for both the fresh and sulfated catalysts. In the UV–vis region, the silver species can be classified into three main features, viz., ions, clusters, and nanoparticles [24]. Each type of silver species possesses a specific absorption wavelength: the region between

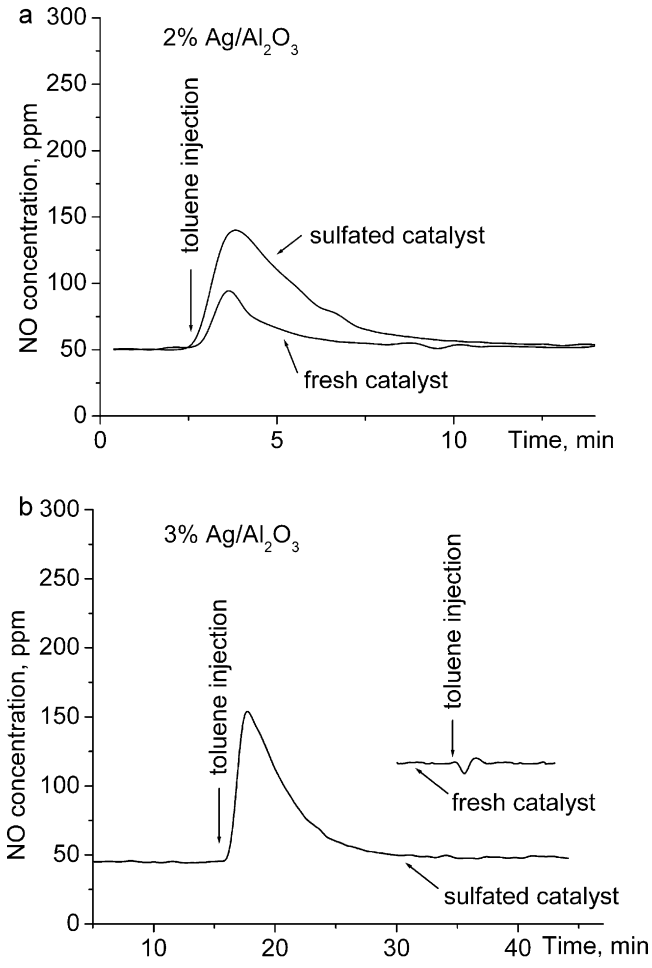

Fig. 7. Effect of 0.01 ml toluene injection on NO reduction over (a) 2% Ag/Al_2O_3 and (b) 3% Ag/Al_2O_3 at 350 °C for fresh and sulfated samples. Initial NO concentration was 300 ppm. Sulfation pretreatment was done at 450 °C for 6 h using 30 ppm SO_2, 7 vol.% H_2O, and 12 vol.% O_2.

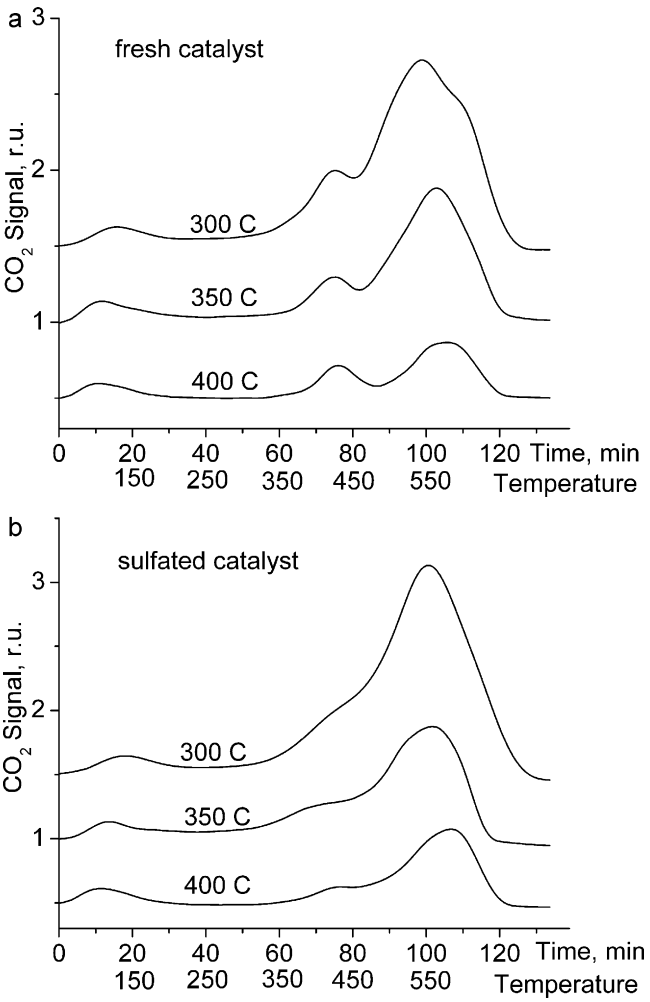

Fig. 9. Temperature-programmed decomposition profiles for used 2% Ag/Al_2O_3 (a) fresh and (b) sulfated samples. Catalyst was tested in SCR reaction mixture of 29% toluene and 71% octane at 300, 350, and 400 °C for 4 h at a flow rate of 200 cm^3/min, initial NO concentration of 300 ppm, and C_1:NO ratio of 6. Sulfation pretreatment conditions are the same as in Fig. 7.

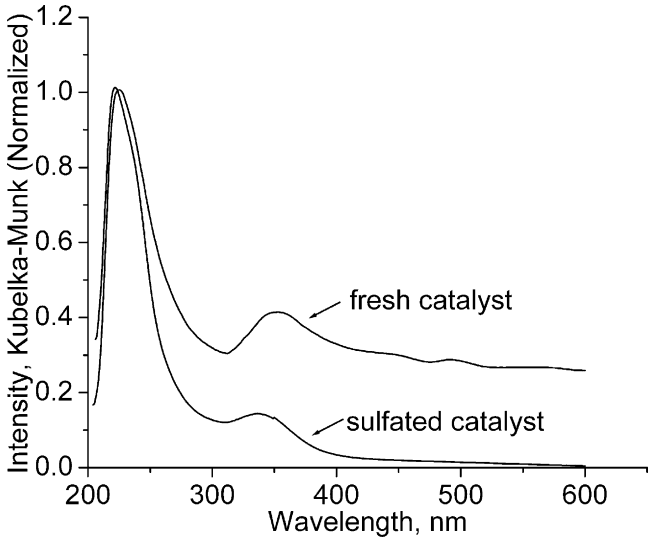

Fig. 8. UV–vis spectra of 3% Ag/Al_2O_3 in 300 ppm NO, 300 ppm CO, 7 vol.% H_2O, 12 vol.% O_2, 6 vol.% CO_2, 225 ppm octane, and balance He at 300 °C for the fresh and sulfated samples. Sulfation pretreatment conditions are the same as in Fig. 7.

190 and 230 nm is assigned to dispersed silver ions on the alumina; clusters containing 2–8 silver atoms are commonly attributed to the absorption bands in the region of 255–390 nm, whereas silver nanoparticles with diameter of ~10 nm give characteristic band in the visible region (>400 nm) [24–26]. It is clear that sulfation mainly results in a decrease in the quantity of large silver particles. We believe that there is an optimum in the silver particle size for HC-SCR. Large silver particles facilitate the partial oxidation of hydrocarbon species at low temperature, and the resulting oxygenate species are critical for NO_x reduction. However, beyond a certain limit, the large silver particles can fully oxidize the hydrocarbon species even before the NO_x reduction begins. Based on our experiments, it appears that sulfur primarily reacts with the large silver particles responsible for partial oxidation of hydrocarbons, and thereby decreases the SCR activity at low temperature and increases it at high temperature.

Besides reacting with the silver particles, sulfur may react with the alumina support as well. The sulfation treatment increases the acidity of the catalyst, as observed in our ammonia TPD tests (not shown). According to literature reports, sulfur (presumably in the form of SO_3) reacts with the alumina support to form aluminum sulfate [14,19], and we believe that it modifies the surface hydrocarbons as well. Fig. 9 shows the TPD profiles for the (a) fresh and (b) sulfated catalysts investigated at different temperatures. In case of

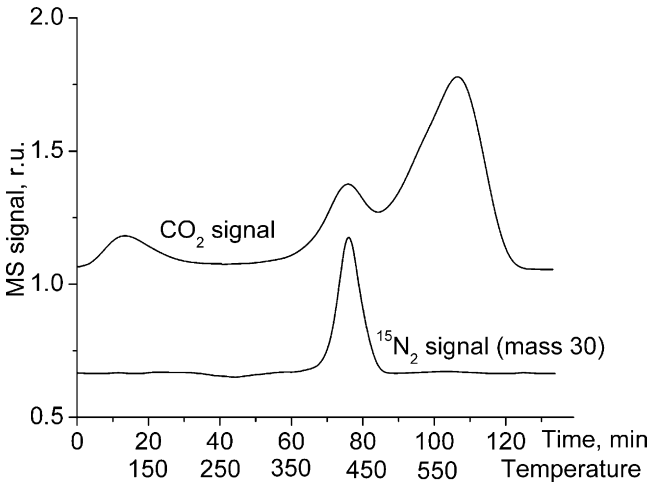

Fig. 10. Nitrogen formation during temperature-programmed decomposition process of the used catalyst. Catalyst was tested in SCR reaction mixture of 29% toluene and 71% octane at 350 °C for 4 h at a flow rate of 200 cm^3/min, initial ^{15}NO concentration of 300 ppm, 300 ppm CO, 7 vol.% H_2O, 12 vol.% O_2, 6 vol.% CO_2, and C_1:NO ratio of 6.

the fresh catalyst (Fig. 9a) tested at 400 °C, two almost similar CO_2 peaks are observed at ~425 °C and ~575 °C, corresponding to two different types of surface hydrocarbon species. Similar experiments at lower temperatures (300 and 350 °C) show an increase in the relative magnitude of the second peak, as it is difficult to oxidize the hydrocarbon species corresponding to high temperature peak at the lower operating temperature. Sulfation modifies the TPD profiles as shown in Fig. 9b, where it is noticeable that the first CO_2 peak is significantly smaller for the sulfated catalyst as compared to the fresh catalyst in Fig. 9a. Therefore, it appears that sulfation increases the relative magnitude of the strongly bound hydrocarbon species, which corresponds to the high temperature peak. In general, the effect of aromatic species is similar to that of sulfur – both decrease the quantity of the low-temperature surface hydrocarbon species and increase the concentration of high-temperature surface hydrocarbon species.

In order to allocate the TPD peaks with the SCR reaction, additional tests were conducted in the presence of isotopically labeled ^{15}NO. Mass 30 was registered as $^{15}N_2$ by mass spectrometer. Fig. 10 shows that nitrogen formation occurs simultaneously with the first CO_2 peak in the TPD profile. Therefore there are at least two types of the oxygen-containing hydrocarbon species on the surface, viz., (1) desired carbon – the species that is involved in the SCR reaction resulting formation of N_2 and (2) undesired carbon – the accumulation of which finally leads to coke formation on the catalyst surface. The presence of aromatic species, sulfation treatment, and lower operating temperature increase the quantity of such undesired carbon and thereby results in catalyst deactivation.

4. Conclusions

Deactivation mechanisms for Ag/Al_2O_3 catalyst due to aromatic species and sulfur in the diesel fuel are explored for HC-SCR of NO_x. Using model hydrocarbon species, such as octane, toluene, and xylene, it is observed that the aromatic species competitively adsorb with alkanes and result in lower catalytic activity. This inhibition effect is reversible and depends on the size and concentration of the aromatic species. Similar experiments for a sulfated catalyst show enhanced inhibition effect due to aromatic species, indicating that the catalyst deactivation due to aromatic species and sulfur is cumulative. Role of sulfur in catalyst deactivation is explored using diffuse reflectance UV–vis and temperature programmed decomposition experiments. It is proposed that sulfur reacts with the large silver particles responsible for partial oxidation of the hydrocarbon species to oxygenates, which are essential for NO_x reduction. Furthermore, sulfur also affects the relative magnitude of the hydrocarbon species adsorbed on the surface – it promotes the undesired carbon, the accumulation of which finally leads to coke formation. In general, catalyst deactivation is enhanced by the presence of aromatic species, catalyst sulfation, and lower operating temperature.

References

[1] R. Burch, Cat. Rev: Sci and Eng. 46 (2004) 271.
[2] U.G. Alkemade, B. Schumann, Solid State Ionics 177 (2006) 2291.
[3] P. Sazama, L. Capek, H. Drobna, Z. Sobalik, J. Dedecek, K. Arve, B. Wichterlova, J. Catal. 232 (2005) 302.
[4] S. Satokawa, J. Shibata, K. Shimizu, A. Satsuma, T. Hattori, Appl. Catal. B: Environ. 42 (2003) 179.
[5] R. Burch, J.P. Breen, F.C. Meunier, Appl. Catal. B: Environ. 39 (2002) 283.
[6] V. Houel, P. Millington, R. Rajaram, A. Tsolakis, Appl. Catal. B: Environ. 73 (2007) 203.
[7] A. Satsuma, K.-I. Shimizu, Prog. Energy Combust. Sci. 29 (2003) 71.
[8] M. Richter, R. Fricke, R. Eckelt, Catal. Lett. 94 (2004) 115.
[9] P. Forzatti, Appl. Catal. A 222 (2001) 221.
[10] A. Satsuma, M. Haneda, T. Fujitani, H. Hamada, Micropor. Mesopor. Mater. 111 (2008) 488.
[11] M. Iwamoto, H. Yahiro, H. Khil-Shin, M. Watanabe, J. Guo, M. Konno, T. Chikahisa, T. Murayama, Appl. Catal. B: Environ. 5 (1994) L1–L5.
[12] C.U.I. Odenbrand, J. Blanco, P. Avila, C. Knapp, Appl. Catal. B: Environ. 23 (1999) 37.
[13] S. Sitshebo, A. Tsolakis, K. Theinnoi, J. Rodríguez-Fernández, P. Leung, Chem. Eng. J. 158 (2010) 402.
[14] J.P. Breen, R. Burch, C. Hardacre, C.J. Hill, B. Krutzsch, B. Bandl-Konrad, E. Jobson, L. Cider, P.G. Blakeman, L.J. Peace, M.V. Twigg, M. Preis, M. Gottschling, Appl. Catal. B: Environ. 70 (2007) 36.
[15] A.B. Mhadeshwar, B.H. Winkler, B. Eiteneer, D. Hancu, Appl. Catal. B: Environ. 89 (2009) 229.
[16] F.C. Meunier, J.R.H. Ross, Appl. Catal. B: Environ. 24 (2000) 23.
[17] N. Hickey, P. Fornasiero, J. Kaspar, M. Graziani, G. Martra, S. Coluccia, S. Biella, L. Prati, M. Rossi, J. Catal. 209 (2002) 271.
[18] H.W. Jen, Catal. Today 42 (1998) 37.
[19] V. Houel, P. Millington, S. Pollington, S. Poulston, R. Rajaram, A. Tsolakis, Catal. Today 114 (2006) 334.
[20] T.N. Angelidis, S. Christoforou, A. Bongiovanni, N. Kruse, Appl. Catal. B: Environ. 39 (2002) 197.
[21] P.W. Park, C.L. Boyer, Appl. Catal. B: Environ. 59 (2005) 27.
[22] T. Nakatsuji, R. Yasukawa, K. Tabata, K. Ueda, M. Niwa, Appl. Catal. B: Environ. 17 (1998) 333.
[23] S. Satokawa, K. Yamaseki, H. Uchida, Appl. Catal. B: Environ. 34 (2001) 299.
[24] H. Bi, W. Bai, C. Kan, L. Zhang, J. Appl. Phys. 92 (2002) 749.
[25] J. Shibata, K. Shimizu, Y. Takada, A. Shichi, H. Yoshida, S. Satokawa, A. Satsuma, T. Hattori, J. Catal. 227 (2004) 367.
[26] M. Richter, U. Bentrup, R. Eckelt, M. Schneider, M.-M. Pohl, R. Fricke, Appl. Catal. B: Environ. 51 (2004) 261.